ELSEVIER

Journal of Power Sources 93 (2001) 156–162

JOURNAL OF POWER SOURCES

www.elsevier.com/locate/jpowsour

Effect of aluminium doping on cathodic behaviour of $LiNi_{0.7}Co_{0.3}O_2$

S. Madhavi[a], G.V. Subba Rao[b,*], B.V.R. Chowdari[b,c], S.F.Y. Li[a,b]

[a]*Department of Chemistry, National University of Singapore, Singapore 119260, Singapore*
[b]*Institute of Materials Research & Engineering, 3 Research Link, Singapore 117602, Singapore*
[c]*Department of Physics, National University of Singapore, Singapore 119260, Singapore*

Received 26 June 2000; accepted 18 August 2000

Abstract

Solid solutions of the formula $LiNi_{0.7}Co_{0.3-z}Al_zO_2$ ($0.0 \leq z \leq 0.20$) have been synthesized and characterized by X-ray diffraction (XRD), scanning electron microscopy (SEM), and surface area and density measurements. Single-phase materials are obtained for $z \leq 0.15$. Their cathodic behaviour in coin cells with Li metal as anode and a liquid electrolyte is examined by charge–discharge cycling at the $0.13C$ rate between 2.7 and 4.3 V and by cyclic voltammetry. Irreversible capacity loss occurs for all the compositions, but the phases with $z = 0.05$ and $z = 0.10$ show much less capacity fading at the end of 50 cycles as compared to those with $z = 0.0$ and $z > 0.10$. The 5 at.% Al-doped compound showed a discharge capacity of 137 mA h^{-1} g after 100 cycles that corresponds to 70% capacity retention. The beneficial effect of Al-doping ($z \leq 0.10$) is corroborated by cyclic voltammograms and differential scanning calorimetry (DSC) data on charged cathodes.

Keywords: Lithium-ion batteries; Cathodes; Aluminium; Nickel; Cobalt

1. Introduction

At present, $LiCoO_2$ is widely used as a cathode material for rechargeable lithium-ion batteries [1–3]. This mixed oxide possesses a layered structure and lithium ions de-intercalate and intercalate during the charge–discharge process, and thus, contribute to the cathodic capacity. Due to the high cost of this oxide, other materials such as $LiNiO_2$, which is isostructural to $LiCoO_2$, are under consideration for cathodes [4]. Unfortunately, synthesis problems, high capacity fading on charge–discharge cycling due to several crystallographic phase transformations and low thermal stability of the oxide in the charged state have inhibited the commercialization of lithium nickel oxide as the preferred cathode [5,6].

In an effort to stabilize the two-dimensional (2D) layered structure of $LiNiO_2$, $LiNi_{1-y}M_yO_2$ phases (where M is a transition or a non-transition metal) have been investigated. Among these substituted compounds, $LiNi_{1-y}Co_yO_2$ compounds are of considerable interest since they form complete solid solutions for all values of y [7–12]. The introduction of increasing amounts of Co into the lattice of $LiNiO_2$ stabilizes the 2D-character of the crystal lattice by reducing the cation mixing (i.e. reduced occupancy of Ni ions in the Li layer) [7]. Studies on the electrochemical behaviour of $LiNi_{1-y}Co_yO_2$ phases have established that, within the range $0.2 \leq y \leq 0.4$, there is a minimal change in the unit cell volume during intercalation and de-intercalation. This implies that $y = 0.2$ and $y = 0.3$ phases give good cycling properties and an ordered 2D-structure of the material enhances the ease of the lithium diffusion in the interslab spaces [8,9]. Delmas et al. [9] also found that, when $LiNi_{1-y}Co_yO_2$/Li cells are cycled between 4.0 and 2.7 V at low currents (0.07–0.4 mA cm^{-2}), the composition with $y = 0.3$ exhibits a better capacity retention than that with $y = 0.2$. This is because of enhanced layer characteristic with increasing Co content. Recent studies by Cho et al. [12] also establish that the $y = 0.3$ composition exhibits a high current rate capability as the cathode.

Other cations, e.g. Mg, Ti, Al, Nb and Ga, have been doped in $LiNiO_2$ and found to improve charge–discharge reversibility, give lower capacity fading, and/or increase thermal stability in the charged (de-intercalated) state [13–24]. Low dopant concentrations ($\leq$5 at.%) of Ga [13], Mg [7,14], Nb or Ca [15] and co-doping with (Ga, Mg) [16], (Ti, Mg) [17] and (Co, Mn) [18,19] in $LiNiO_2$ exhibit improved electrochemical characteristics of the compound by suppressing the phase transformations. Aluminium has been of continuous interest as a substituent in

* Corresponding author. Fax: +65-872-0785.
E-mail address: gv-sr@imre.org.sg (G.V. Subba Rao).

0378-7753/01/$ – see front matter
PII: S0378-7753(00)00559-0

$LiCoO_2$ and $LiNiO_2$ cathodes due to its low atomic mass and low cost. Ohzuku and coworkers [22,23] have investigated the structural changes of $LiNi_{3/4}Al_{1/4}O_2$ during the charge–discharge process via ex situ X-ray diffraction (XRD) and have shown that a single hexagonal phase is preserved over the entire range of Li content. This feature is beneficial in terms of long cycle-life of the electrode. $LiNi_{3/4}Al_{1/4}O_2$ is also found to be thermally more stable compared to $LiNiO_2$ in the charged state. Doping of an electrochemically inactive species like Al into $LiNiO_2$ intrinsically limits the maximum amount of Li that can be de-intercalated and intercalated depending on the Al content. Hence, doping prevents the cell from overcharge, and thus, improves the safety characteristics [22,23]. The work of Wang et al. [24] substantiated the beneficial effects of Al-doped $LiNiO_2$. Theoretical calculations by Ceder and coworkers [25,26], and subsequent experimental verification by Jang et al. [27,28], and Huang et al. [29] have indeed shown that Al substitution at the Co sites in $LiCoO_2$ increases the cell voltage but gives reasonably good cathodic capacity and decreases both the cost and the density of the material.

In the present study, the effect of an additional dopant, namely Al, on the cathodic behaviour of the $LiNi_{0.7}Co_{0.3}O_2$ phase is investigated. The synthesis, characterization and electrochemical behaviour of a series of Al-doped compounds, $LiNi_{0.7}Co_{0.3-z}Al_zO_2$ ($0.0 \leq z \leq 0.20$), are reported. Results show that capacity fading is significantly suppressed for $z = 0.05$ and 0.10 and thermal stability in the charged state is improved.

2. Experimental

The mixed oxides $LiNi_{0.7}Co_{0.3-z}Al_zO_2$ ($0.0 \leq z \leq 0.20$) were synthesized in 10–15 g batches by heating stoichiometric mixtures of high-purity raw materials, NiO (BDH), Co_3O_4 (Merck), $Al(OH)_3$ (Merck) and $LiNO_3$ (Alfa) first at 300°C for 5 h and then at 750°C for 20 h in a flowing oxygen atmosphere using a tubular furnace (Carbolite, UK), followed by slow cooling (1°C min^{-1}) to room temperature. Preliminary heating at 300°C enables the $LiNO_3$ to melt and impregnate other raw materials, and thus, ensures more uniform distribution of the salt before the thermal decomposition to form the mixed oxide. Powder XRD was used to identify the crystalline phase (Siemens D5005, Cu $K\alpha_1$ radiation). The XRD patterns were indexed and lattice parameters calculated using least-squares fitting. The BET surface area of the powder samples was measured by means of a Micromeritics, USA, Model Tristar 3000 unit. The bulk density was determined with a Micromeritics, USA, Model Accupyc 1330 unit which uses the helium displacement method. Scanning electron microscopic (SEM) micrographs were taken with a Philips XL30 instrument at various magnifications to study the particle morphology.

Galvanostatic charge–discharge cycling tests were performed on two-electrode coin cells with lithium metal foil as the anode. A 1:1 (v/v) mixture of ethylene carbonate (EC) and dimethyl carbonate (DMC) containing 1 M $LiPF_6$ was used as the electrolyte (Merck). A slurry was made from the oxide material, Super P carbon black as the conducting additive and polyvinylidene difluoride (PVDF) as a binder (in the weight ratio 80:10:10) in NMP solvent. Electrodes were fabricated by applying the slurry to an Al foil (25 μm thick) using a paint applicator and drying it in an air oven at 80°C to evaporate the solvent. The foil was then pressed between rollers at a pressure of 5–8 tonnes and dried in a vacuum oven to ensure that the electrode was free from moisture and solvent. The foil was cut into circular strips of 16 mm diameter. Coin-type test cells (size 2016) were assembled, using polypropylene (Celgard) as the separator, in an argon-filled dry box (MB150B-G, MBraun, USA) which maintained the contents of O_2 and H_2O to <1 ppm. The open-circuit voltage (OCV) of freshly fabricated cells was in the range 3.0–3.5 V.

Charge–discharge tests and cyclic voltammograms were performed with computer-controlled, multi-channel, battery testing units (Bitrode, USA; Macpile, Biologic, France and EG&G, USA, Model 263A). Differential scanning calorimetry (DSC) measurements were carried out on the cathode samples by charging the coin cells to 4.3 V at a 0.1*C* rate followed by holding them at the same potential for 20 h. The cell were then disassembled. The cathode material was scrapped off and a weighed amount was sealed in an Al-sample holder. Thermal studies were carried out with a DSC system supplied by TA Instruments, USA (Model 2010) in the range 100–350°C at a heating rate of 3°C min^{-1}.

3. Results and discussion

The compounds are black in colour and stable towards exposure to air and moisture. Nevertheless, they were stored in a desiccator to prevent reduction and decomposition. The XRD patterns of $LiNi_{0.7}Co_{0.3-z}Al_zO_2$ ($0.0 \leq z \leq 0.20$) show the formation of single phase with a well-defined layer structure (α-$NaFeO_2$ type; rhombohedral–hexagonal structure with the space group R $\bar{3}$m). No impurity phases are seen in this range of doping. The intensity ratio of (0 0 3) and (1 0 4) peaks in the XRD patterns is greater than unity and there is a clear splitting of the (0 0 6) and (1 0 2), (1 0 8) and (1 1 0) doublet peaks in all the compounds which confirms that there is no cation mixing in the layered structure (Table 1). Slow-scan XRD patterns (Fig. 1) in the regions corresponding to the mixed (*h k l*) reflections, viz. (1 0 1) and (0 0 6) and (1 0 2) doublet peaks, reveal a symmetrical nature of the peaks for $z \leq 0.15$. This indicates that the solid-state reaction method presently employed in the synthesis of the compounds yields homogenous phases and there is no phase separation [7]. The XRD pattern of a $z = 0.2$ composition (Fig. 1) showed a slightly unsymmetrical (1 0 1) peak which indicated that there might be a small amount of inhomogeneity in the distribution of Al in the (Ni, Co)-

Table 1
Physical and cathodic capacity data of the compounds $LiNi_{0.7}Co_{0.3-z}Al_zO_2$ ($0 \leq z \leq 0.2$)

z	Intensity ratio (0 0 3/1 0 4)	a (A)	c (A)	Density (g cm^{-3})		Cathodic capacity (mA h g^{-1})			
				Experimental	Calculated	Initial charge	Initial discharge	Irreversible loss in the first cycle	Discharge capacity retention (1st–50th cycle) (%)
0.0	1.54	2.855	14.15	4.74	4.88	215	180	35	72
0.05	1.34	2.862	14.17	4.62	4.76	228	198	30	78[a]
0.10	1.21	2.862	14.16	4.53	4.69	219	168	51	84
0.125	1.32	2.861	14.19	4.50	4.64	243	188	55	62
0.15	1.26	2.862	14.21	4.47	4.59	188	139	49	72
0.20	1.17	2.863	14.20	4.36	4.51	187	130	57	–

[a] Cycling tests were extended up to 100 cycles. Measured discharge capacity is 137 mA h g^{-1} and corresponds to 70% capacity retention.

layer in the crystal lattice. The hexagonal lattice parameters a and c for the undoped compound $LiNi_{0.7}Co_{0.3}O_2$ are found to be 2.855 and 14.15 A, respectively. These are in very good agreement with values reported ($a = 2.86$ A, $c = 14.16$ A) for the same composition by Delmas et al. [9]. The a and c lattice parameters remain almost unchanged with increasing amount of Al dopant, as can be expected from the ionic radii of the elements ($Ni^{3+} = 0.560$ A, $Co^{3+} = 0.545$ A, $Al^{3+} = 0.535$ A; octahedral coordination: low spin Ni and Co). The c/a ratio in all the compounds with various z values were found to be in the range 4.95–4.96, as expected for a 2D-layer structure [9–12]. We note that, for a lattice with large cation mixing, the c/a ratio will be 4.89–4.91. The measured densities (Table 1) correspond to 97–98% of the theoretical values which are calculated from the crystal lattice parameters. The decrease in density of the material with increase in the Al dopant is due to the lower atomic mass of the dopant (Table 1). The BET surface area of the samples ranges from 0.50 to 1.50 m^2 g^{-1}. This indicates the well-sintered nature of the oxide particles. Electron micrographs of the powder samples show agglomerated particles with a size of 12–18 μm and platelet morphology.

Galvanostatic charge–discharge curves have been recorded for the $LiNi_{0.7}Co_{0.3-z}Al_zO_2$ ($0.0 \leq z \leq 0.15$) cathode materials at a current rating of 0.13C up to 50 cycles. The current rating is calculated from the actual current employed (0.2 mA), the weight of the active material and an assumed theoretical capacity of 192 mA h g^{-1}. The cathodes were initially charged to 4.5 V (versus Li metal) to ensure complete oxidation of the Ni ions in the lattice.

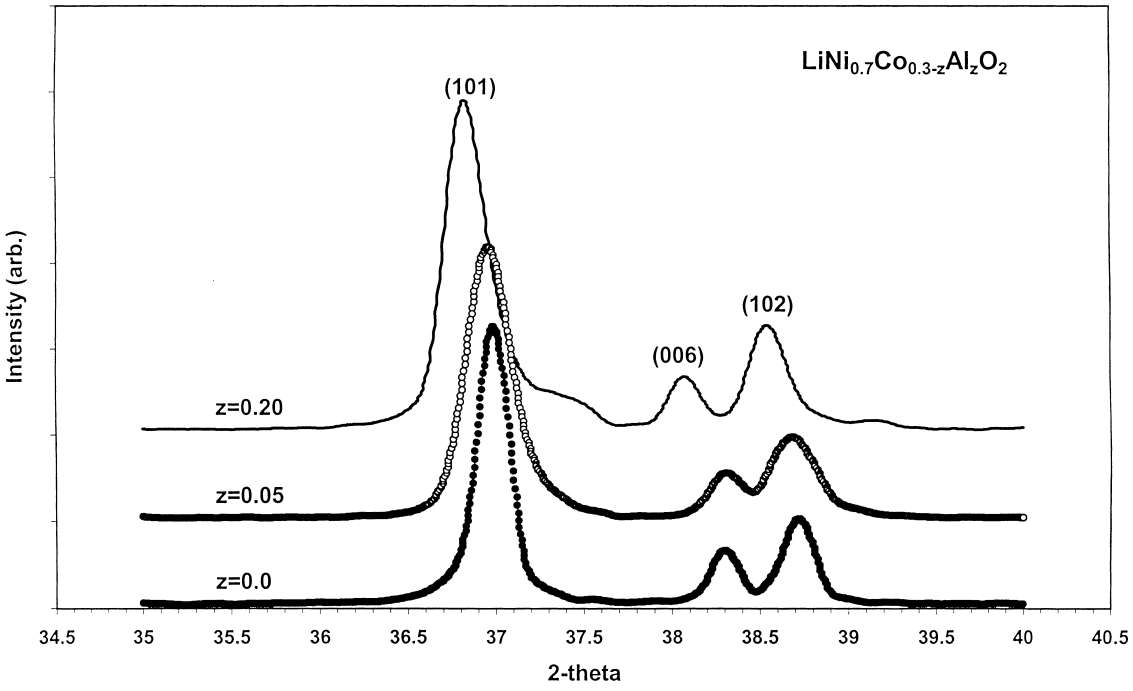

Fig. 1. Slow-scan XRD patterns of $Li(Ni_{0.7}Co_{0.3-z}Al_z)O_2$ ($z = 0.00$, 0.05 and 0.20) in the region corresponding to the (h k l) reflections (1 0 1), (0 0 6) and (1 0 2). Symmetric peaks observed for $z = 0.00$ and 0.05 demonstrate the single-phase nature of the compounds. Unsymmetrical (1 0 1) peak for $z = 0.20$ shows slight inhomogeneity in Al distribution in the lattice.

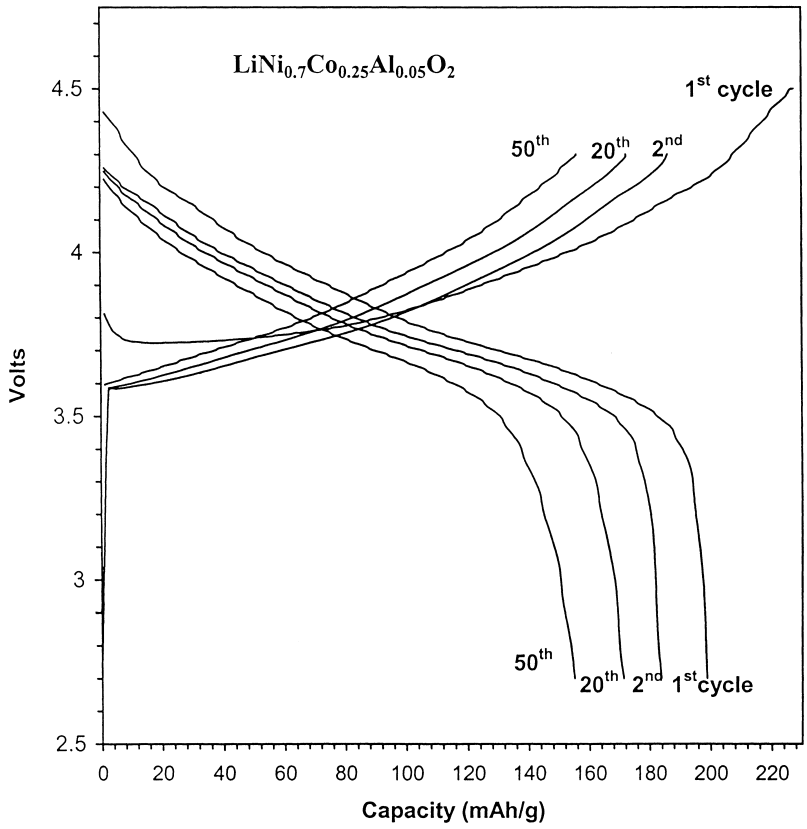

Fig. 2. Representative charge–discharge curves of $Li(Ni_{0.7}Co_{0.25}Al_{0.05})O_2$ ($z = 0.05$) at 0.13C rate in voltage window; 2.7–4.3 V (versus Li). First charge taken up to 4.5 V. The differences in charge–discharge capacities are within 1% from the 2nd to the 50th cycle, indicating excellent reversibility. Capacity retention is 78% after 50 cycles, calculated from the first discharge capacity. See also Table 1.

Due to the high voltage applied, partial oxidation of some of the Co^{3+} to Co^{4+} ions also occurs and this contributes to the cathodic first-charge capacity. After the first discharge to a cut-off voltage of 2.7 V, from the second cycle onwards, the cells were cycled in a voltage window of 2.7–4.3 V. The relevant data are presented in Table 1. Representative charge–discharge curves for the $z = 0.05$ composition are shown in Fig. 2.

All the compounds showed an irreversible loss of capacity between the first charge and first discharge. The actual values depend on the Al content. While the value is 35 mA h g^{-1} for $z = 0$, it falls to 30 mA h g^{-1} for $z = 0.05$, but lies in the range 49–55 mA h g^{-1} for $z = 0.10$–0.15 (Table 1). The capacity loss is a general phenomenon which is exhibited by almost all the Ni^{3+}-containing cathodes [4,7,9–12,16,17,19]. Delmas and coworkers [7,10] ascribed this capacity loss to the formation of electrochemically inactive regions in the cathode due to the oxidation of pre-existing Ni^{2+} ions which occupy the Li layer. In the compounds examined here, the values are slightly high. This is obviously due to the high initial charging voltage (4.5 V). For all the compositions, from the second cycle onwards, we note that there is almost no difference in the charge and discharge capacity values. This shows that the coulombic efficiency is very high ($\geq$98%), as can be seen from Fig. 2 for the representative $z = 0.05$ composition.

The discharge capacity for various compositions as a function of the number of cycles is presented in Fig. 3. The values for the $z = 0.05$ compound consistently remain higher than those for other z values, including $z = 0.0$. For the $z = 0.05$ composition, data were obtained up to 100 cycles at which the discharge capacity is 137 mA h g^{-1} and

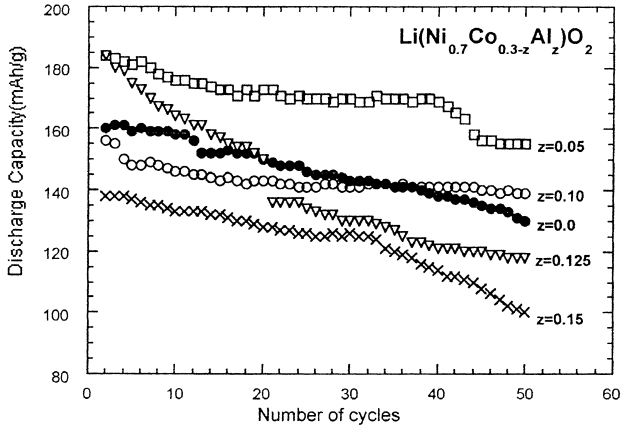

Fig. 3. Discharge capacity vs. number of charge–discharge cycles of $Li(Ni_{0.7}Co_{0.3-z}Al_z)O_2$ ($z = 0.00$–0.15) at the 0.13C rate in the voltage window 2.7–4.3 V (vs. Li). The $z = 0.05$ composition consistently shows higher capacity. Capacity retention for $z = 0.10$ composition improves after 35 cycles as compared to $z = 0.00$.

corresponds to 70% retention of the initial discharge capacity. As can be seen from Table 1 and Fig. 3, the capacity retention after 50 cycles is higher for $z = 0.05$ and 0.1. From the relative variation of the slopes of the curves in Fig. 3, it can be concluded that the $z = 0.05$ and 0.10 compounds display the best cathodic behaviour and are definitely superior to the $z = 0.0$ composition. These two compositions are now being tested for high-rate capability. For the $z = 0.20$ composition, the initial discharge capacity is ≅130 mA h g^{-1}, but there is a rapid fall in the performance with further cycling. This might be attributed to the phase inhomogeneity of the Al distribution already present in the compound, as seen from the slow-scan XRD (Fig. 1), which degrades the reversible intercalation and de-intercalation of Li in the lattice. Also, due to the dilution effect of electrochemically inactive Al, the electronic conductivity of the cathode decreases with increasing z, and thereby affects the current pick-up.

Cyclic voltammograms (*i*/*V* curves) have been recorded for the various cathodic compositions using coin-type cells with Li metal as the reference/counter electrode to gain insight in to the phase transitions which take place during the charge–discharge process. Representative *i*/*V* curves for $z = 0.0$ and 0.05 are shown in Fig. 4. The curves on the first cycle (virgin) differ from those on the second and subsequent cycles with respect to the voltage ranges in which the oxidation–reduction (Li de-intercalation–intercalation) reactions occur. This is due to the large irreversible loss of capacity and activation of the electrode on contact with the electrolyte. From the second or third cycle onwards, the curves overlap excellently. This indicates the quantitative reversibility of the electrode reactions. Suppression of the phase transitions in $LiNi_{0.7}Co_{0.3}O_2$, compared to pure $LiNiO_2$, is confirmed by the absence of well-defined spikes at various voltages in the *i*/*V* curves. A broad maximum at 3.9–4.1 V in the oxidation region and a broad minimum at 3.2–3.4 V in the reduction region are observed for the compound with $z = 0.0$. A broad shoulder in the cathodic curve at 4.2 V is also clearly seen (Fig. 4b). Delmas et al. [7] reported that in these Co-doped compositions, second-order (order–disorder type) phase transitions exist during the removal and addition of Li. These are reflected as broad peaks in the derivative curves (dx/dV versus x (or V)) which are extracted from the galvanostatic charge–discharge or GITT curves [3,7,19]. Thus, cyclic voltammograms are complimentary to the above two techniques. The observations are in general agreement with those reported by Cho et al. [12]. The Al-doped ($z = 0.05$) composition shows the same general *i*/*V* behaviour as that of $z = 0.0$, but the maximum and minimum and the shoulder peaks (in the

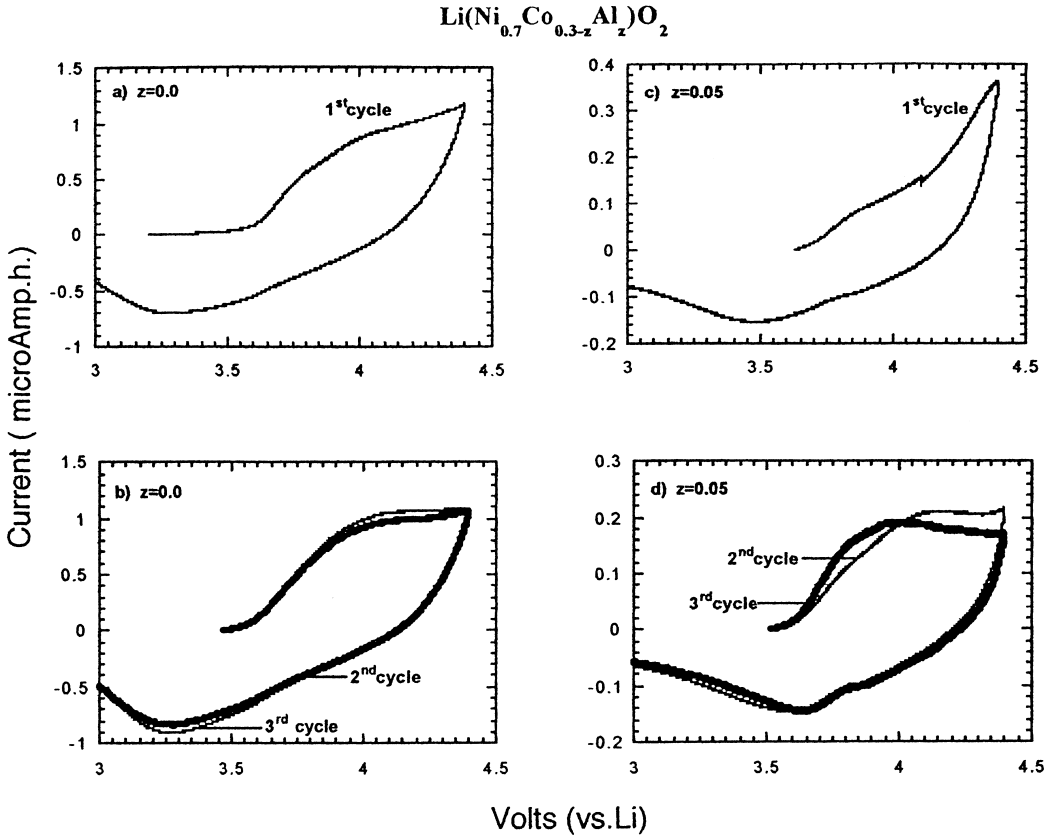

Fig. 4. Cyclic voltammograms for $Li(Ni_{0.7}Co_{0.3-z}Al_z)O_2$, $z = 0.00$ (a and b) and $z = 0.05$ (c and d). Coin-type cell with Li metal as reference/counter electrode. The voltage range is 3.0–4.4 V at a scan rate of 0.05 mV s^{-1}. Curves for the first cycle are different from those for the second and subsequent cycles. The broad anodic and cathodic peaks are indicative of suppression of phase transitions in $LiNiO_2$ by substitution of Co and Al.

reduction curve) are more prominent. Further, the broad minimum in the cathodic curve is shifted to higher voltage, namely, 3.6–3.7 V, and an additional shoulder is observed at 3.85 V. The anodic peak position is shifted to a lower value (3.9–4.0 V). Significantly, the hysteresis in the voltage decreases from 0.7 to 0.35 V for $z = 0.0$ and 0.05, respectively. This is an indication of improved charge–discharge reversibility and Li-ion mobility of the electrode. The hysteresis value observed for $z = 0.125$ from *i/V* curves (not shown) is 0.5–0.6 V and the general shape of the curve, as expected, resembles that for the $z = 0.05$ composition. We can conclude that the *i/V* data corroborate our earlier findings that the $z = 0.05$ and 0.10 compositions perform much better than those with $z = 0.0$ and $z = 0.125$ in yielding higher cathodic capacities and lower capacity fading at least up to 50 cycles.

Improved Li-ion mobility in the crystal lattice and capacity retention upon Al-doping can be understood in a qualitative fashion by consideration of the structural and the bonding aspects. For small values of z (0.05–0.10), the Al ions will occupy the (Ni, Co)-layer in $LiNi_{0.7}Co_{0.3-z}O_2$ and are randomly distributed. Since the Al–O bond is more ionic than the Co–O bond, it will make the Ni–O bonds more covalent and will thereby increase the ionicity of the Li–O bond, and consequently, increase the mobility of lithium ions in the Li layer. Also, the randomly distributed and electrochemically inactive Al ions will suppress any tendency for the ordering of Ni ions in the Ni layer and the ordering of Li ion vacancies in the Li layer. It is well known that poor cycleability or capacity fading in the cathode is related to the 2D nature during charge–discharge cycling. In the range $x = 0.0$–0.5 in $Li_{1-x}CoO_2$, the 2D nature of the lattice is retained, and thus, the compound shows excellent cycleability. $LiNiO_2$, on the other hand, undergoes several phase transitions (hexagonal → monoclinic → hexagonal) due to the ordering of Li ions and/or vacancies in the range $x = 0.0$–0.65 in $Li_{1-x}NiO_2$ during charging (and reversibly during the discharge process) [6–9,30], and thus, the degree of 2D nature decreases during these phase transitions. Simultaneous substitution by cobalt and aluminium is able to retain the 2D nature of the lattice by effectively suppressing or eliminating the ordering of the Li ions/vacancies. Also, the smaller ionic size of Al^{3+} compared to Co^{3+} is a favourable factor. We note that, in the voltage window presently employed, viz. 2.7–4.3 V, only the Ni^{3+} ions will participate in the charge–discharge process. The Co^{3+} ions, along with the Al^{3+} ions, will play a passive but effective role in retaining the degree of 2D nature of the lattice and contribute to better cycleability.

DSC studies were carried out after charging the cells to 4.3 V at the 0.1*C* rate to evaluate the effect of Al content on the thermal stability of the charged cathode. A characteristic sharp exothermic peak (T_d) was observed for $LiNi_{0.7}Co_{0.3}O_2$ ($z = 0.0$) at 222°C which agrees well with the observations of Cho et al. [12]. With increasing amounts of Al dopant, this peak shifts slightly towards higher temperatures, as shown in Fig. 5. The values in the *y*-axis scale have been normalized with respect to the active weight of the cathode material. As can be seen, the area under the peak shrinks enormously with increasing amounts of Al dopant, whereas the T_d values

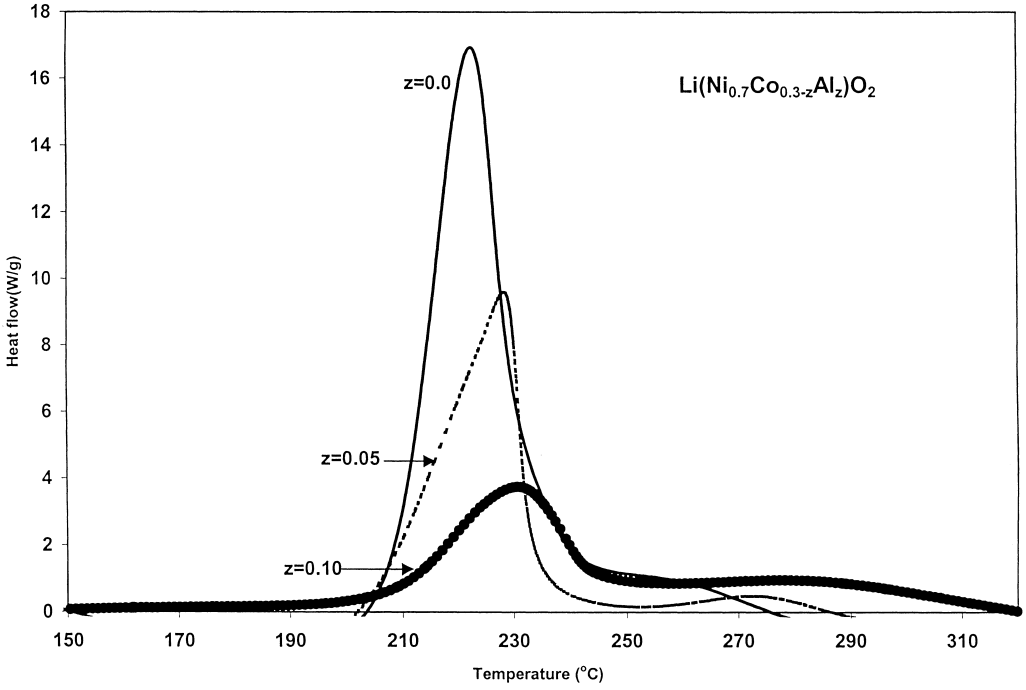

Fig. 5. DSC curves of the charged cathodes $Li(Ni_{0.7}Co_{0.3-z}Al_z)O_2$, where $z = 0.00$, 0.05, 0.10. Cells charged to 4.3 V at the 0.1*C* rate, equilibrated for 20 h at 4.3 V and then disassembled. Curves are normalized to the weight of the cathode active material. The area under the curve decreases with increasing value of z, but temperatures (T_d) are only slightly shifted (from 222 to 230°C).

increase slightly, to 230°C. This shows the improved thermal stability of these Al-doped materials in the fully charged state, even though the decomposition temperatures have not increased much. It is known that a fully-charged cathode containing Ni^{4+} ions in the lattice evolves oxygen at T_d via an exothermic decomposition reaction [3,12,16,17,31]. Al-doping is able to reduce the overall heat effect (decreased peak area at T_d) because of better heat dissipation. Since aluminium oxide (Al_2O_3) is an excellent thermal conductor compared to Ni or Co oxide, it can be concluded that Al^{3+} ions doped in Li(Ni, Co)O_2 assist dissipation of the heat arising from the decomposition from the Ni^{4+} centres.

4. Conclusions

Aluminium has been substituted at the Co sites in $LiNi_{0.7}Co_{0.3}O_2$ to form uniform solid solutions of the composition $LiNi_{0.7}Co_{0.3-z}Al_zO_2$ ($0.0 < z < 0.15$). High values of z ($\geq$0.20) lead to cation mixing and the formation of other impurity phases. These compounds show improved electrochemical cycling behaviour as the cathode material for Li-ion batteries. The $z = 0.05$ and $z = 0.10$ phases show higher capacity and less capacity fading up to 50 cycles compared to the $z = 0.0$ phase. The $z = 0.05$ composition shows a capacity of 137 mA h g^{-1} which corresponds to 70% capacity retention after 100 cycles at the 0.13C rate in the voltage range 2.7–4.3 V. Cyclic voltammograms corroborate these findings. The addition of Al dopant improves the thermal stability of the material, and thus, contributes to the improved safety of the cathodic material in the charged state. Present studies show that $0.05 \leq z \leq 0.10$ in $LiNi_{0.7}Co_{0.3-z}Al_zO_2$ is the optimum level of Al dopant to provide the beneficial effects.

Acknowledgements

The authors thank Dr. H.J. Lindner for his interest in the progress of the work. Thanks are also due to Ms. Doreen Lai and Mr. Rasid Ali (IMRE) for technical support.

References

[1] R. Koksbang, J. Barker, H. Shi, M.Y. Saidi, Solid State Ionics 84 (1996) 1.
[2] R. Alcantara, P. Lavela, J.L. Tirado, E. Zhecheva, R. Stoyanova, J. Solid State Electrochem. 3 (1999) 121.
[3] M. Broussely, P. Biensan, B. Simon, Electrochim. Acta 45 (1999) 3.
[4] T. Ohzuku, A. Ueda, M. Nagayama, J. Electrochem. Soc. 140 (1993) 1862.
[5] M. Broussely, F. Perton, J. Labat, J. Power Sources 43/44 (1993) 209.
[6] C. Delmas, J.P. Peres, A. Rougier, A. Demourgues, F. Weill, A. Chadwick, M. Broussely, F. Perton, Ph. Biensan, P. Willmann, J. Power Sources 68 (1997) 120.
[7] C. Delmas, M. Menetrier, L. Croguennec, I. Saadoune, A. Rougier, C. Pouillerie, G. Prado, M. Grune, L. Fournes, Electrochim. Acta 45 (1999) 243.
[8] C. Delmas, I. Saadoune, Solid State Ionics 53–56 (1992) 370.
[9] C. Delmas, I. Saadoune, A. Rougier, J. Power Sources 43/44 (1993) 595.
[10] I. Saadoune, C. Delmas, J. Mater. Chem. 6 (1996) 193.
[11] J. Cho, G. Kim, H.S. Lim, J. Electrochem. Soc. 146 (1999) 3571.
[12] J. Cho, H. Jung, Y. Park, G. Kim, H.S. Lim, J. Electrochem. Soc. 147 (2000) 15.
[13] Y. Nishida, K. Nakane, T. Satoh, J. Power Sources 68 (1997) 561.
[14] C. Louchet, C. Delmas, Ph. Biensan, P. Willmann, in: Paper presented at IMLB-9, Edinburgh, UK, July 1998.
[15] Y. Sato, T. Koyano, M. Mukai, K. Kobayakawa, Denki Kagaku (Japan) 66 (1998) 1215.
[16] A. Yu, G.V. Subba Rao, B.V.R. Chowdari, Solid State Ionics, 2000, in press.
[17] Y. Gao, M.V. Yakovleva, W.B. Ebner, Electrochem. Solid-State Lett. 1 (1998) 117.
[18] Z. Liu, A. Yu, J.Y. Lee, J. Power Sources 81/82 (1999) 416.
[19] H. Arai, S. Okada, Y. Sakurai, J. Yamaki, J. Electrochem. Soc. 144 (1997) 3117.
[20] Q. Zhong, A. Bonakdarpour, M. Zhang, Y. Gao, J.R. Dahn, J. Electrochem. Soc. 144 (1997) 205.
[21] M.E. Spahr, P. Novak, B. Schnyder, O. Haas, R. Nesper, J. Electrochem. Soc. 145 (1998) 1113.
[22] T. Ohzuku, A. Ueda, M. Kouguchi, J. Electrochem. Soc. 142 (1995) 4033.
[23] T. Ohzuku, T. Yanagawa, M. Kouguchi, A. Ueda, J. Power Sources 68 (1997) 131.
[24] G.X. Wang, S. Zhong, D.H. Bradhurst, S.X. Dou, H.K. Liu, Solid State Ionics 116 (1999) 271.
[25] G. Ceder, Y.M. Chiang, D.R. Sadoway, M.K. Aydinol, Y.I. Jang, B. Huang, Nature (London) 392 (1998) 694.
[26] G. Ceder, M.K. Aydinol, A.F. Kohan, Comput. Mater. Sci. 8 (1997) 161.
[27] Y.I. Jang, B. Huang, H. Wang, D.R. Sadoway, G. Ceder, Y.M. Chiang, H. Liu, H. Tamura, J. Electrochem. Soc. 146 (1999) 862.
[28] Y.I. Jang, B. Huang, H. Wang, G.R. Maskaly, G. Ceder, D. Sadoway, Y.M. Chiang, H. Liu, H.J. Tamura, J. Power Sources 81/82 (1999) 589.
[29] H. Huang, G.V. Subba Rao, B.V.R. Chowdari, J. Power Sources 81/82 (1999) 690.
[30] J.P. Peres, F. Weill, C. Delmas, Solid State Ionics 116 (1999) 19.
[31] Ph. Biensan, B. Simon, J.P. Peres, A. de Guibert, M. Broussely, J.M. Bodet, F. Perton, J. Power Sources 81/82 (1999) 906.